

Velocity space scattering coefficients with applications in antihydrogen recombination studies

Yongbin Chang and C. A. Ordonez

Department of Physics, University of North Texas, Denton, Texas 76203

(Received 2 June 2000)

An approach for calculating velocity space friction and diffusion coefficients with Maxwellian field particles is developed based on a kernel function derived in a previous paper [Y. Chang and C. A. Ordonez, *Phys. Plasmas* **6**, 2947 (1999)]. The original fivefold integral expressions for the coefficients are reduced to onefold integrals, which can be used for any value of the Coulomb logarithm. The onefold integrals can be further reduced to standard analytical expressions by using a weak coupling approximation. The integral expression for the friction coefficient is used to predict a time scale that describes the rate at which a reflecting antiproton beam slows down within a positron plasma, while both species are simultaneously confined by a nested Penning trap. The time scale is used to consider the possibility of achieving antihydrogen recombination within the trap. The friction and diffusion coefficients are then used to derive an expression for calculating the energy transfer rate between antiprotons and positrons. The expression is employed to illustrate achieving antihydrogen recombination while taking into account positron heating by the antiprotons. The effect of the presence of an electric field on recombination is discussed.

PACS number(s): 52.25.Dg, 52.25.Wz, 52.25.Fi

I. INTRODUCTION

Velocity space friction and diffusion coefficients are the lower order coefficients in the Fokker-Planck equation and are useful for, for example, evaluating time scales that are governed by velocity space scattering. The Fokker-Planck equation and the associated coefficients are described in Ref. [1], where historical references can also be found. For weakly coupled plasmas, plasmas with a Coulomb logarithm larger than ten, only the lower order terms of the expansion of the Fokker-Planck equation need to be kept. In addition, the assumption of weak coupling provides the convenience of allowing the lower order Fokker-Planck coefficients to be approximated using analytical expressions when the field particles are Maxwellian. However, there exist many laboratory and astrophysical plasmas that are not weakly coupled [2], and some collision terms for nonweakly coupled plasmas have been developed. The third order term of the Fokker-Planck equation has been derived [2]. Fokker-Planck coefficients of arbitrarily high orders have been developed and have been presented as a unified expression [3]. The Boltzmann collision integral has been expanded to fourth order terms, and the importance of close collision events has been emphasized [4]. In addition, some effort has gone into improving the description of the binary collision mechanics in plasmas [5] and the accuracy of the Coulomb logarithm for nonweakly coupled plasmas [6,7].

In principle, the complete Fokker-Planck equation is expressed as the following infinite series [8,9]:

$$\left(\frac{\partial f}{\partial t}\right)_{\text{coll}} = \sum_{N=1}^{\infty} \frac{(-1)^N}{N!} \frac{\partial^N}{\partial \mathbf{v}^N} \langle \Delta \mathbf{v}^N \rangle f. \quad (1)$$

The Fokker-Planck equation gives the time rate of change of the distribution function f due to collisions. In Eq. (1), $\Delta \mathbf{v}^N$ is the N th order dyad of velocity change for the test particle and the Fokker-Planck coefficients $\langle \Delta \mathbf{v}^N \rangle$, which are aver-

ages per unit time, are defined in terms of a probability function $P(\mathbf{v}, \Delta \mathbf{v})$ as follows [9,10]:

$$\langle \Delta \mathbf{v}^N \rangle = \int \Delta \mathbf{v}^N P(\mathbf{v}, \Delta \mathbf{v}) d\Delta \mathbf{v}. \quad (2)$$

In Sec. II, a derivation of the probability function for Maxwellian field particles is presented. The probability function is used in Sec. III to obtain onefold integral expressions for the Fokker-Planck friction and diffusion coefficients. The integrals are over the range of possible changes in momentum for a test particle undergoing binary Coulomb collisions with field particles. The integrals are exact but diverge due to the long range Coulomb interaction. Approximations are necessarily introduced when a nonzero lower integration limit is chosen to avoid the divergence. The lower limit is evaluated in terms of the Coulomb logarithm in Sec. IV. In Sec. V, the correspondence of the present theory with prior theory is shown. A weak coupling approximation is applied to the onefold integrals to obtain standard analytical expressions. The present theory is not restricted in applicability, at least for evaluating velocity space scattering effects due to binary Coulomb collisions. For example, the present theory can be applied when the Coulomb logarithm has a value less than 10. In Sec. VI, the suitability of some expressions for the Coulomb logarithm are considered for small Coulomb logarithm values. As an application of the present theory, a time scale is predicted that describes the rate at which antiprotons slow down within a positron plasma. In Sec. VII, the time scale is used to consider the possibility of achieving antihydrogen recombination when both the antiprotons and positrons are simultaneously confined within a nested Penning trap. The present theory is also used to derive an expression for the rate at which energy is transferred from the antiprotons to the positrons. In Sec. VIII, the expression is presented and then used to assess the effect that antiproton heating of the positrons has on achieving antihydrogen re-

combination. A discussion regarding the effect of an electric field on recombination is presented in Sec. IX. Concluding remarks are given in Sec. X.

II. DERIVATION OF PROBABILITY FUNCTION FOR MAXWELLIAN FIELD PARTICLES

To obtain an expression for the probability function in Eq. (2), the Fokker-Planck coefficients can be written in terms of an integral over a scattering cross section. For Maxwellian field particles, the Fokker-Planck coefficients have been written as [9,10]

$$\langle \Delta \mathbf{v}^N \rangle = \int \Delta \mathbf{v}^N f_M(\mathbf{v}_F) g \sigma_R \sin \theta d\theta d\phi d\mathbf{v}_F, \quad (3)$$

where

$$\sigma_R = \left(\frac{zz_F e^2}{4\pi\epsilon_0\mu} \right)^2 \frac{1}{4g^4 \sin^4(\theta/2)} \quad (4)$$

is the Rutherford cross section, $f_M(\mathbf{v}_F)$ is the Maxwellian velocity distribution for the field particles, $\mu = mm_F/(m + m_F)$ is the reduced mass, θ is the scattering angle in the center-of-mass system, ϕ is the azimuthal angle around the relative velocity $\mathbf{g} = \mathbf{v} - \mathbf{v}_F$, \mathbf{v} and \mathbf{v}_F are the velocities of the test particle and field particle, z and z_F are the charge states of the test and field particle, m and m_F are the masses of the test and field particle, e is the unit charge, and ϵ_0 is the permittivity of free space. It is possible to start with Eq. (3) and then change Eq. (3) into the form of Eq. (2) by using a variable change technique [3,11–13]. Changing the integration variables from $(\mathbf{v}_F, \theta, \phi)$ to $(\Delta \mathbf{v}, \theta, \phi')$, Eq. (3) provides

$$\langle \Delta \mathbf{v}^N \rangle = \int \Delta \mathbf{v}^N f_M(\mathbf{v}_F) g \sigma_R \sin \theta |J| d\theta d\phi' d\Delta \mathbf{v}, \quad (5)$$

where J is the Jacobian for the change of variables and ϕ' is the azimuthal angle around $\Delta \mathbf{v}$. Comparing Eq. (2) and Eq. (5), the probability function is written

$$P(\mathbf{v}, \Delta \mathbf{v}) = \int f_M(\mathbf{v}_F) g \sigma_R \sin \theta |J| d\theta d\phi'. \quad (6)$$

To implement the approach, a kernel function is defined: $C = f_M(\mathbf{v}) P(\mathbf{v}, \Delta \mathbf{v})$. Here $f_M(\mathbf{v})$ is a function introduced to simplify the integral in C . The integral in C is evaluated in Ref. [11] and found to be

$$C = nn_F \left(\frac{\sqrt{mm_F}}{2\pi a k T} \right)^3 \frac{v_{th} \pi d^2}{u_\delta} \exp\left(\frac{\epsilon_\gamma^2}{u_\delta^2} - 2\epsilon_\chi - u_\delta^2 \right) \quad (7)$$

using

$$f_M(\mathbf{v}) = n \left(\frac{m}{2\pi k T} \right)^{3/2} \exp\left(-\frac{mv^2}{2kT} \right), \quad (8)$$

where $\epsilon_\chi = \mathbf{v} \cdot \mathbf{v}' / (av_{th}^2)$, $\epsilon_\gamma = |\mathbf{v} \times \mathbf{v}'| / (av_{th}^2)$, $\mathbf{u}_\delta = \Delta \mathbf{v} / (av_{th})$, $a = 2\mu/m$, $d = b/u_\delta^2$, $b = zz_F e^2 m_F / (8\pi\epsilon_0 \mu k T)$, $\Delta \mathbf{v} = \mathbf{v}' - \mathbf{v}$, $v_{th} = \sqrt{2kT/m_F}$ is the thermal speed of the field particles, n_F and T are the density and temperature of the

field particles, n is a constant that factors out, and k is Boltzmann's constant. With this, the probability function is

$$P(\mathbf{v}, \Delta \mathbf{v}) = \frac{n_F v_{th} \pi d^2}{(\sqrt{\pi} a v_{th})^3 u_\delta} \exp\left(\frac{|\mathbf{u} \times \mathbf{u}_\delta|^2}{u_\delta^2} - u^2 - u_\delta^2 - 2\mathbf{u} \cdot \mathbf{u}_\delta \right), \quad (9)$$

where $\mathbf{u} = \mathbf{v} / v_{th}$.

III. SIMPLIFICATION OF FOKKER-PLANCK COEFFICIENTS WITHOUT THE WEAK COUPLING APPROXIMATION

Introducing $(\mathbf{e}_\parallel, \mathbf{e}_{\perp 1}, \mathbf{e}_{\perp 2})$ as an orthogonal triplet of unit vectors with $\mathbf{e}_\parallel = \mathbf{v} / v$, \mathbf{u}_δ is expressed as

$$\begin{aligned} \mathbf{u}_\delta &= u_\delta \mathbf{e}_\parallel + u_{\delta \perp 1} \mathbf{e}_{\perp 1} + u_{\delta \perp 2} \mathbf{e}_{\perp 2} \\ &= u_\delta (\mathbf{e}_\parallel \cos \chi + \mathbf{e}_{\perp 1} \sin \chi \cos \Psi + \mathbf{e}_{\perp 2} \sin \chi \sin \Psi), \end{aligned} \quad (10)$$

where χ is the angle between \mathbf{u}_δ and \mathbf{u} , Ψ is the azimuthal angle of \mathbf{u}_δ around \mathbf{u} , and \parallel , $\perp 1$, and $\perp 2$ denote the direction parallel and two directions perpendicular to \mathbf{u} . It is convenient to change the integration variables in Eq. (2) using the following differential:

$$d\Delta \mathbf{v} = (av_{th})^3 d\mathbf{u}_\delta = (av_{th})^3 u_\delta^2 \sin \chi d\Psi d\chi du_\delta. \quad (11)$$

Equation (2) becomes

$$\begin{aligned} \langle \Delta \mathbf{v}^N \rangle &= (av_{th})^N \langle \mathbf{u}_\delta^N \rangle \\ &= (av_{th})^N \int \mathbf{u}_\delta^N p(\mathbf{u}, \mathbf{u}_\delta) u_\delta^2 \sin \chi d\Psi d\chi du_\delta, \end{aligned} \quad (12)$$

where $p(\mathbf{u}, \mathbf{u}_\delta) = (av_{th})^3 P(\mathbf{v}, \Delta \mathbf{v})$. Defining

$$\tau = \frac{1}{n_F v_{th} \pi b^2}, \quad (13)$$

Eq. (9) is used to obtain

$$p(\mathbf{u}, \mathbf{u}_\delta) = \frac{1}{\pi^{3/2} \tau u_\delta^5 \exp(u_\delta + u \cos \chi)^2}. \quad (14)$$

In Ref. [3], the function $p(\mathbf{u}, \mathbf{u}_\delta)$ is expressed in the form of an infinity series, which is convenient for the calculation of the Fokker-Planck coefficients for $N \geq 3$. For completeness, higher order, $N \geq 3$, Fokker-Planck coefficients are listed here. They are [3]

$$\begin{aligned} &\langle \Delta v_\parallel^{N-2(J+K)} \Delta v_{\perp 1}^{2J} \Delta v_{\perp 2}^{2K} \rangle \\ &= \frac{\beta(J+1/2, K+1/2)}{(-1)^{J+K} \pi} \sum_{i=0}^{J+K} C_{J+K}^i \\ &\times \sum_{j=L}^{N-i-1} \frac{\Gamma(3/2+L-i)}{\Gamma(3/2-M+j)} C_{M-i}^{j-L} F_{N,i,j}(u^2), \end{aligned} \quad (15)$$

where β and Γ are the beta and gamma functions, L equals the greatest integer less than or equal to $(N-1)/2$, and M equals the greatest integer less than or equal to $N/2$. The function $F_{N,i,j}$ is defined as

$$F_{N,i,j}(x) = \frac{(-1)^{N+i}(av_{\text{th}})^N x^{j+1-N/2} [x^j e^x \gamma^*(3/2-i+j, x)]^{(j)}}{\tau e^x j}, \quad (16)$$

where γ^* is a form of the incomplete gamma function [14],

$$\gamma^*(\alpha, x) = \frac{1}{x^\alpha \Gamma(\alpha)} \int_0^x e^{-t} t^{\alpha-1} dt. \quad (17)$$

In the present work, new expressions for lower order ($N < 3$) Fokker-Planck coefficients are derived. The field particles are assumed to have an isotropic Maxwellian velocity distribution, and

$$\langle \Delta v^2 \rangle = \langle \Delta v_{\parallel}^2 \rangle + \langle \Delta v_{\perp 1}^2 \rangle + \langle \Delta v_{\perp 2}^2 \rangle, \quad (18)$$

$$\langle \Delta v_{\perp 1}^2 \rangle = \langle \Delta v_{\perp 2}^2 \rangle, \quad (19)$$

and

$$\langle \Delta v_{\perp 1} \rangle = \langle \Delta v_{\perp 2} \rangle = 0. \quad (20)$$

Hence the friction coefficient $\langle \Delta v_{\parallel} \rangle$ and two diffusion coefficients $\langle \Delta v_{\parallel}^2 \rangle$ and $\langle \Delta v^2 \rangle$ can be considered the independent coefficients. Applying Eq. (12) to the three coefficients, substituting in Eq. (14), integrating over Ψ , changing the integration variables from χ to $x = \cos \chi$, and integrating over x yields

$$\langle \Delta v_{\parallel} \rangle = \frac{av_{\text{th}}}{\tau u^2} \int \frac{e^{-W^2} - e^{-U^2} - \sqrt{\pi} u_{\delta} [\text{erf}(U) + \text{erf}(W)]}{\sqrt{\pi} u_{\delta}^2} du_{\delta}, \quad (21)$$

$$\langle \Delta v^2 \rangle = \frac{(av_{\text{th}})^2}{\tau u} \int \frac{[\text{erf}(U) + \text{erf}(W)]}{u_{\delta}} du_{\delta}, \quad (22)$$

and

$$\langle \Delta v_{\parallel}^2 \rangle = \frac{(av_{\text{th}})^2}{\tau u^3} \int \frac{-We^{-U^2} - Ue^{-W^2} + \sqrt{\pi} \left(\frac{1}{2} + u_{\delta}^2 \right) [\text{erf}(U) + \text{erf}(W)]}{\sqrt{\pi} u_{\delta}} du_{\delta}, \quad (23)$$

where $U = u + u_{\delta}$, $W = u - u_{\delta}$, and erf is the error function.

IV. INTEGRATION LIMITS AND THE COULOMB LOGARITHM

No approximations are used to arrive at Eqs. (21)–(23) and the equations apply without restrictions. For example, the test particle speed can be larger than the thermal speed of the field particles. Unfortunately, approximations are necessarily introduced when the limits of integration are chosen. In order to take into account all possible binary Coulomb collisions, the limits of integration for Eqs. (21)–(23) are $u_{\delta, \text{min}} = 0$ and $u_{\delta, \text{max}} = \infty$. However, setting the lower limit of integration equal to zero causes the integrals to diverge as a result of the long range of the Coulomb interaction. Because $u_{\delta} = m\Delta v / (2\mu v_{\text{th}})$ is proportional to the magnitude of the change in the test-particle momentum $\Delta p = m\Delta v$ due to a Coulomb collision, it is necessary to define a lower cutoff in the range of values Δp may have. To proceed further, u_{δ} is written in terms of an associated impact parameter ρ and a limited range of impact parameters is considered. For a binary Coulomb collision

$$u_{\delta} = \frac{g}{v_{\text{th}} \sqrt{1 + \rho^2 / \beta^2}}, \quad (24)$$

where $\beta = z z_F e^2 / (4\pi \epsilon_0 \mu g^2)$ is half the classical distance of closest approach for a head-on collision. To write the integration limits $u_{\delta, \text{min}}$ and $u_{\delta, \text{max}}$ in terms of maximum and

minimum impact parameters, ρ_{max} and ρ_{min} , a value must be chosen for the relative speed g . In reality, g has a range of values between zero and infinity. However, if the integration limits are written in terms of maximum and minimum impact parameters, then the same value must be used to replace g in both integration limits so that the integrals in Eqs. (21)–(23) vanish in the limit $\rho_{\text{max}} \rightarrow \rho_{\text{min}}$. A reasonable choice for replacing g is $\langle g \rangle$, the average value of g . For Maxwellian field particles

$$\langle g \rangle = \frac{v_{\text{th}} e^{-u^2}}{\sqrt{\pi}} + v_{\text{th}} \left(u + \frac{1}{2u} \right) \text{erf}(u). \quad (25)$$

Alternative choices for replacing g are v_{th} , which is within 12% of $\langle g \rangle$ for $v < 0.1v_{\text{th}}$, and v , which is within 12% of $\langle g \rangle$ for $v > 2v_{\text{th}}$.

Incorporation of a minimum impact parameter may be useful for taking into account quantum effects [7] and the effects of particle sink reactions such as fusion reactions [15]. Here, $\rho_{\text{min}} = 0$ is used to allow ρ_{max} to be written in terms of the Coulomb logarithm in a simple way. The Coulomb logarithm is defined [6]

$$\lambda = \frac{1}{2\pi\beta^2} \int \sin^2 \left(\frac{\theta}{2} \right) \left(\frac{d\sigma}{d\Omega} \right) d\Omega, \quad (26)$$

where Ω is the scattering solid angle in the center of mass frame and $d\sigma/d\Omega$ is the differential scattering cross section.

Assuming azimuthally random collisions, the Coulomb logarithm is equivalently defined by

$$\lambda = \frac{1}{\beta^2} \int_{\pi}^0 \sin^2\left(\frac{\theta}{2}\right) \left(\frac{d\sigma}{d\Omega}\right) \sin\theta d\theta \quad (27)$$

or alternatively by

$$\lambda = \frac{1}{\beta^2} \int_0^{\infty} \sin^2\left(\frac{\theta}{2}\right) \rho d\rho, \quad (28)$$

where $d\Omega = 2\pi \sin\theta d\theta$ and $d\sigma = 2\pi\rho d\rho$ are used.

For a classical binary Coulomb collision, the center-of-mass scattering angle is related to the impact parameter by $\sin^2(\theta/2) = 1/(1 + \rho^2/\beta^2)$ or equivalently by $\rho = \beta \cot(\theta/2)$. The associated differential scattering cross section, which is known as the Rutherford cross section, is $d\sigma/d\Omega = \sigma_R = -(\beta/2)^2 \csc^4(\theta/2)$. Integrating from $\theta = \pi$ to $\theta = 2 \arcsin(1/\sqrt{1 + \rho_{\max}^2/\beta^2})$ or from $\rho = 0$ to $\rho = \rho_{\max}$ provides

$$\lambda = \ln\left(\sqrt{1 + \frac{\rho_{\max}^2}{\beta^2}}\right). \quad (29)$$

Solving for ρ_{\max} , substituting into Eq. (24), and replacing g by its average provides the lower integration limit

$$u_{\delta,\min} = \frac{\langle g \rangle e^{-\lambda}}{v_{\text{th}}}. \quad (30)$$

The corresponding upper integration limit is obtained by substituting $\rho = \rho_{\min} = 0$ into Eq. (24) and replacing g by its average:

$$u_{\delta,\max} = \frac{\langle g \rangle}{v_{\text{th}}}. \quad (31)$$

Writing the lower integration limit in terms of the Coulomb logarithm allows different Coulomb logarithm expressions to be used in the theory. It should be kept in mind, however, that Eq. (29) is the only Coulomb logarithm expression that is truly consistent with the present theory for $\rho_{\min} = 0$.

V. FRICTION AND DIFFUSION COEFFICIENTS WITH WEAK COUPLING ASSUMPTION

Assuming that the dominant contribution to friction and diffusion come from weak collision events, a Taylor series expansion of the integrands in Eqs. (21)–(23) may be done. The usual form of the friction and diffusion coefficients are recovered by keeping only the lowest order terms in the expansion, and by considering $\langle g \rangle = v_{\text{th}}$ and the corresponding integration limits $u_{\delta,\min} = e^{-\lambda}$ and $u_{\delta,\max} = 1$. With the definition of Chandrasekhar's function [1,9]

$$G(x) = \frac{1}{2} \left(\frac{\text{erf}(x)}{x^2} - \frac{2e^{-x^2}}{\sqrt{\pi}x} \right), \quad (32)$$

the friction and diffusion coefficients are reduced to

$$\langle \Delta v_{\parallel} \rangle = -\frac{4av_{\text{th}}\lambda G(u)}{\tau}, \quad (33)$$

$$\langle \Delta v^2 \rangle = \frac{2(av_{\text{th}})^2 \lambda \text{erf}(u)}{\tau u}, \quad (34)$$

and

$$\langle \Delta v_{\parallel}^2 \rangle = \frac{2(av_{\text{th}})^2 \lambda G(u)}{\tau u}, \quad (35)$$

which are standard analytical expressions [9,16]. These expressions agree to within 5% with Eqs. (21)–(23) for Coulomb logarithm values larger than 10 and test particle speeds less than the thermal speed of the field particles ($u < 1$) when the integration limits $u_{\delta,\min} = e^{-\lambda}$ and $u_{\delta,\max} = 1$, are used in Eqs. (21)–(23).

VI. COULOMB LOGARITHM FOR SMALL COULOMB LOGARITHM VALUES

A comparison is presented in Ref. [17] between theory and experimental anisotropic temperature relaxation rate data. The experimental data was obtained using non-neutral plasmas, in which the cyclotron radius r_c was smaller than the Debye length λ_D [18,19]. Theory that employed the usual form for the Coulomb logarithm

$$\lambda = \ln \Lambda, \quad (36)$$

was found to agree with the experimental data reported in Ref. [18] for $\Lambda \gg 1$ with $\Lambda = 1/(0.333\kappa)$ where $\kappa = 2\sqrt{2}\beta/r_c$ and β equals half the classical distance of closest approach. A numerical treatment was used to determine the numerical factor 0.333. Note that considering the cyclotron radius as the maximum impact parameter yields $\Lambda = \rho_{\max}/(0.666\sqrt{2}\beta) = 1.06\rho_{\max}/\beta \approx \rho_{\max}/\beta$.

The experimental data reported in Ref. [18] are associated with Λ values much larger than unity. The experimental data in Ref. [19] are associated with values of Λ closer to unity and include values both larger and smaller than unity. (Nevertheless, the experimental data in Ref. [19] are from weakly correlated plasmas.) The numerical treatment reported in Ref. [17] agrees with the experimental data reported in Ref. [19] to within the estimated experimental error. A function denoted $I(\kappa)$ was calculated using the numerical treatment, and a spectrum of values are reported in Tables I and II of Ref. [17]. The numerical treatment was developed considering an adiabatic invariant that governs the equipartition rate between parallel and perpendicular (to the magnetic field) velocity components. For $\kappa \ll 1$ ($\Lambda \gg 1$), the equipartition rate is the same in both “magnetized” ($r_c < \lambda_D$) and “unmagnetized” ($r_c \gg \lambda_D$) plasmas (with λ_D replaced by r_c in the Coulomb logarithm when $r_c < \lambda_D$), and the correspondence between the Coulomb logarithm and $I(\kappa)$ is given by [17]

$$\lambda = \frac{15I(\kappa)}{\sqrt{2}\pi}. \quad (37)$$

For velocity space scattering due to binary collisions within an unmagnetized plasma, the physics associated with

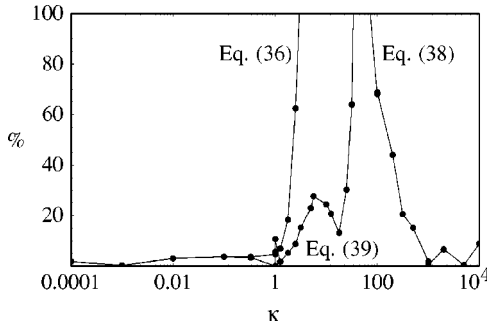


FIG. 1. Comparison of three analytical expressions, Eqs. (36), (38), and (39), for the Coulomb logarithm. Shown is the percentage that each expression is different from each numerical value. The points are joined by three lines to guide the eye.

the collision dynamics of a test particle is contained within the Coulomb logarithm [6]. For a magnetized plasma, the function $I(\kappa)$ takes into account all dependence on the magnetic field strength [17]. In the present work, a Coulomb logarithm for magnetized plasmas is defined using Eq. (37) by hypothesis. The hypothesis is consistent with the procedure used in Ref. [17] for carrying out comparisons with experimental data. The procedure was equivalent to replacing the Coulomb logarithm within theory for unmagnetized plasmas using Eq. (37) and using the cyclotron radius for the maximum impact parameter.

An expression for $I(\kappa)$ is provided in Ref. [17] that is suitable for $\kappa \gg 1$ ($\Lambda \ll 1$). Employing the definition given by Eq. (37), the corresponding Coulomb logarithm is written as

$$\lambda = \frac{15}{\sqrt{2\pi}} \exp\left[\frac{-5(3\pi\kappa)^{2/5}}{6}\right] (1.83\kappa^{-7/15} + 20.9\kappa^{-11/15} + 0.347\kappa^{-13/15} + 87.8\kappa^{-1} + 6.68\kappa^{-17/15}). \quad (38)$$

In Fig. 1 of Ref. [15], a comparison of theory (for unmagnetized plasmas but using the cyclotron radius for the maximum impact parameter) and the anisotropic temperature relaxation rate experimental data from Ref. [19] is shown. Approximate agreement (within 69% for all but one data point) was found when

$$\lambda = \ln(\sqrt{1 + \Lambda^2}) \quad (39)$$

was used for the Coulomb logarithm. The values of the Coulomb logarithm extended from 0.00015 to 6.5. Note that Eqs. (29) and (39) are the same when $\Lambda = \rho_{\max}/\beta$.

Figure 1 shows the difference, expressed as a percentage, between the analytical expressions, Eqs. (36), (38), and (39), and numerical values obtained from Tables I and II of Ref. [17] using Eq. (37). Equations (36) and (39) are calculated using $\Lambda = 1/(0.333\kappa)$. Equations (36), (38), and (39) are found to agree to within 30% with the numerical values for $\kappa < 1.78$ ($\lambda > 0.6$), $\kappa > 316$ ($\lambda < 5 \times 10^{-9}$), and $\kappa < 25$ ($\lambda > 0.006$), respectively. For $25 < \kappa < 316$ ($5 \times 10^{-9} < \lambda < 0.006$),

$$\lambda = \left(\frac{1}{\lambda_{38}} + \frac{1}{\lambda_{39}}\right)^{-1} \quad (40)$$

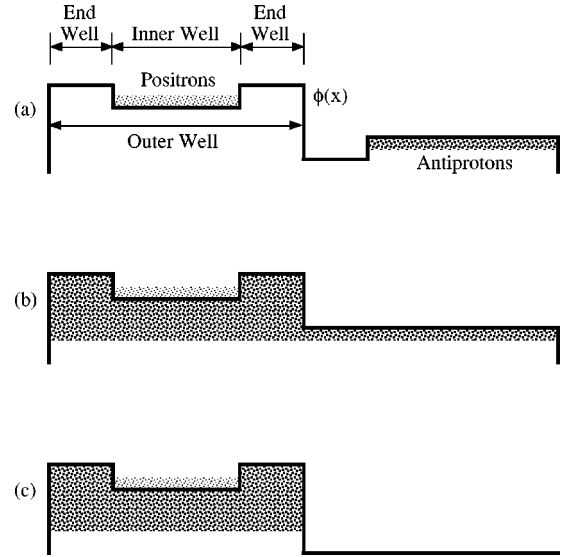


FIG. 2. Illustration of a method for achieving overlap of antiprotons and positrons within a nested Penning trap.

(not shown in Fig. 1) agrees to within 59% with the numerical values where λ_{38} and λ_{39} denote the expressions given by Eqs. (38) and (39).

VII. ANTIHYDROGEN APPLICATION

The year 2000 is expected to mark the beginning of an international effort to produce low-energy antihydrogen atoms for scientific study [20–22]. The attempts will commence at the CERN AD (Antiproton Decelerator) facility and the use of nested Penning traps to achieve antihydrogen recombination is planned. (The reader is referred to Refs. [23–25] for more details on plasma confinement in nested Penning traps and to Refs. [20–22] for more details on the expected operating parameters for achieving antihydrogen recombination.) Here, a method is considered for achieving overlap of a positron plasma by a reflecting antiproton beam within a nested Penning trap such that recombination occurs. The method has been explored experimentally using electrons and protons although recombination was not reported [26]. Figure 2 illustrates the method. Initially, positrons and antiprotons are stored in separate potential wells [Fig. 2(a)]. The potential profile is produced using cylindrical electrodes that are aligned along a magnetic field. The magnetic field provides radial confinement of the charged particles. The antiprotons are allowed to flow into a lower potential energy “outer well” [Fig. 2(b)] and then are captured within the outer well [Fig. 2(c)]. The change in potential energy experienced by the antiprotons is much larger than their thermal energy, so they can be regarded as forming a reflecting beam. The reflecting antiproton beam passes through the positron plasma, which is trapped within the “inner well.” Recombination occurs between the antiprotons and positrons while the overlap persists. Recombined antihydrogen atoms form two oppositely directed beams that travel away from the overlap region parallel to the magnetic field.

Two time scales characterize the evolution of the system after the overlap commences. One time scale characterizes the rate at which antiprotons slow down to subsequently be-

come trapped within the “end wells” where the positrons do not reside. The slowing time scale is approximately

$$\tau_s = \frac{v}{|\langle \Delta v_{\parallel} \rangle|}. \quad (41)$$

By way of example, the antiproton slowing time scale is predicted using the present theory for a positron density and temperature of $n_F = 5 \times 10^{13} \text{ m}^{-3}$ and $T = 10 \text{ K}$, and a $B = 2 \text{ T}$ magnetic field. For antiproton speeds larger than about twice the positron thermal speed (antiproton kinetic energies larger than about 6 eV for a positron temperature of 10 K), the overlap is susceptible to the two-stream instability. For the calculation, 3 eV antiprotons are considered. The counterstreaming antiprotons are not susceptible to the two-stream instability themselves provided the condition $n < \pi^2 \epsilon_0 m v^2 / (e \ell)^2$ is satisfied where n and ℓ are the antiproton density and length. (See Ref. [27] for more details on considering the two-stream instability in nested Penning traps.) If the inner well is much longer than the end wells, the condition can be applied to the inner well. For example, for an inner well length of 10 cm, the antiproton density must be less than $3.3 \times 10^{11} \text{ m}^{-3}$.

The positron cyclotron radius r_c is smaller than the Debye length and $\Lambda = r_c / \beta = 0.126$ is used where the numerator and denominator are calculated using $r_c = \sqrt{m_F k T / (e B)} = 3.50 \times 10^{-8} \text{ m}$ and $\beta = z z_F e^2 / (4 \pi \epsilon_0 \mu \langle g \rangle^2) = 2.78 \times 10^{-7} \text{ m}$ with $\langle g \rangle = 3.02 \times 10^4 \text{ m/s}$ given by Eq. (25). With $\kappa = 1 / (0.333 \Lambda) = 23.8$, Eq. (39) is used to obtain $\lambda = 0.00788$. Using Eq. (21) with the integration limits given by Eqs. (30) and (31), the time scale is predicted to be $\tau_s = 0.48 \text{ s}$. In comparison, Eq. (33), which is not expected to be accurate for small Coulomb logarithm values, gives $\tau_s = 0.11 \text{ s}$.

A second time scale characterizes the recombination rate of antihydrogen. Two recombination reactions for forming antihydrogen from free antiprotons and positrons are spontaneous radiative recombination SRR and three-body recombination TBR. The SRR reaction rate coefficient α^{SRR} for a 1 K antihydrogen plasma can be found in Ref. [20]. The associate time scale is $\tau^{\text{SRR}} = 1 / (\alpha^{\text{SRR}} n_F) = 100 \text{ s}$. For a 10 K antihydrogen plasma, the time scale will be even larger. The TBR reaction rate coefficient can be expressed as [28] $\alpha^{\text{TBR}} = 6 \times 10^{-24} (4.2/T)^{9/2} n_F$. This recombination rate pertains to zero magnetic field. For infinitely high fields, the rate will be an order of magnitude less [29]. So the TBR time scale is estimated to be $\tau^{\text{TBR}} \approx 10 / (\alpha^{\text{TBR}} n_F) = 0.033 \text{ s}$. With $\tau^{\text{TBR}} \ll \tau_s$, a substantial fraction of the antiprotons can recombine with positrons to form antihydrogen atoms during the time the overlap persists. It should be noted, however, that newly recombined atoms in highly excited states are susceptible to electric field ionization. Although a study that considered the effect of electric fields on antihydrogen production has been reported [30], more detailed studies that consider both radial and axial electric fields produced under specific operating conditions are needed. For the present configuration, recombined atoms will initially be exposed to the radial electric field produced by the plasma. Afterward the atoms travel axially and pass through the electric field produced by the trap electrodes.

VIII. EFFECT OF POSITRON HEATING ON RECOMBINATION

When a test particle travels through a plasma, an exchange of energy occurs between the test particle and the plasma. For energetic antiprotons traveling through a cold positron plasma, the antiprotons transfer energy to the positrons and cause the positron temperature to increase. The increase in positron temperature, in turn, causes a decrease in the three-body recombination rate between positrons and antiprotons. In the present section, the effect that positron heating has on achieving antihydrogen recombination is assessed.

The average rate at which energy is transferred from a test particle (e.g., an antiproton) to field particles (e.g., positrons) is

$$\frac{dE}{dt} = -\frac{1}{2} m (\langle \Delta v^2 \rangle + 2v \langle \Delta v_{\parallel} \rangle). \quad (42)$$

Substituting Eqs. (21) and (22) into Eq. (42) yields

$$\begin{aligned} \frac{dE}{dt} = & -\frac{mav_{\text{th}}^2}{2\pi u} \\ & \times \int \frac{2e^{-w^2} - 2e^{-U^2} + \sqrt{\pi} u_{\delta} (a-2) [\text{erf}(U) + \text{erf}(W)]}{\sqrt{\pi} u_{\delta}^2} \\ & \times du_{\delta}, \end{aligned} \quad (43)$$

where the integration limits are given by Eqs. (30) and (31). To assess the effect of positron heating, the positron plasma is modeled as having a spatially uniform density n_F and temperature T within a constant confinement volume V_F . In addition, the number of confined positrons is assumed to be much larger than the number of confined antiprotons, and n_F is considered to remain essentially constant. The antiproton plasma is modeled as having a uniform density n , the same diameter as the positron plasma, and a larger constant confinement volume V , which completely encompasses V_F . It is possible for the antiprotons to have an essentially uniform density axially provided that their average axial kinetic energy is much larger than the change in their potential energy between an end well and the inner well [23]. The total power that goes into heating the positron plasma is

$$P_F = n V_F \frac{dE}{dt}, \quad (44)$$

where $n V_F$ equals the number of antiprotons within the overlap volume. Neglecting other possible energy sources and sinks, the positron temperature time dependence due to antiproton heating is given by

$$\frac{dT}{dt} = \frac{2P_F}{3kn_F V_F} = \frac{2n}{3kn_F} \frac{dE}{dt}, \quad (45)$$

where $n_F V_F$ equals the number of confined positrons.

The rate the antiproton density changes due to recombination is

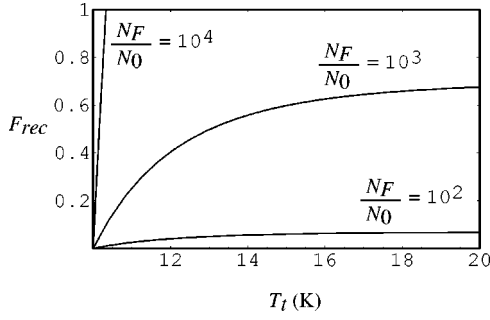


FIG. 3. Effect of antiproton heating of positrons on the fraction F_{rec} of antiprotons that recombine. The positron temperature increases from 10 K to T_t . Each curve is for a different ratio of the number of confined positrons to the initial number of confined antiprotons.

$$\frac{dn}{dt} = -\frac{nn_F\alpha_{\text{rec}}V_F}{V}, \quad (46)$$

where α_{rec} is the total recombination reaction rate coefficient, which can be chosen to include the effects of magnetic and electric fields, collisions, recombination enhancements (e.g., by laser stimulation), etc. It is possible to simplify the problem significantly, however, by using $\alpha_{\text{rec}} = \alpha^{\text{TBR}}/10 = 6 \times 10^{-25} n_F (4.2/T)^{9/2}$, which considers three-body recombination and the adverse effect of the magnetic field. Eliminating n gives

$$-\frac{dn}{dt} = \frac{3kn_F^2\alpha_{\text{rec}}V_F}{2V(dE/dt)} \frac{dT}{dt}. \quad (47)$$

Substituting in the expression for α_{rec} and integrating provides

$$n_0 - n_t = \frac{6 \times 10^{-22} kn_F^3 V_F}{V} \int_{T_0}^{T_t} \frac{dT}{T^{9/2} (dE/dt)}, \quad (48)$$

where subscript 0 denotes an initial value and subscript t denotes a time-elapsed value. Dividing through by n_0 yields an expression for the fraction of antiprotons that recombine as a function of the time-elapsed positron temperature. The expression is

$$F_{\text{rec}} = \frac{6 \times 10^{-22} kn_F^2 N_F}{N_0} \int_{T_0}^{T_t} \frac{dT}{T^{9/2} (dE/dt)}, \quad (49)$$

where $N_F = n_F V_F$ is the number of confined positrons and $N_0 = n_0 V$ is the initial number of confined antiprotons. To evaluate F_{rec} , the antiproton kinetic energy is assumed to remain essentially unchanged during recombination. The same parameters as in the previous section ($n_F = 5 \times 10^{13} \text{ m}^{-3}$, $B = 2 \text{ T}$, and a 3 eV antiproton kinetic energy) are used to calculate F_{rec} and the results are shown in Fig. 3. Each curve indicates the fraction of antiprotons that recombine as a function of the positron temperature. An initial positron temperature of 10 K is assumed, and three curves are shown for three different ratios of the number of confined positrons to the initial number of confined antiprotons. For a ratio equal to 10^4 , all of the antiprotons recombine with the positron temperature increasing by less than 1

K. Such a ratio appears possible. If 10^4 antiprotons are confined, 10^8 positrons would be needed if a positron density of $5 \times 10^{13} \text{ m}^{-3}$ is employed. An accumulation of 3×10^8 positrons with a density of $2 \times 10^{13} \text{ m}^{-3}$ and a cylindrical radius of 3 mm has been reported [31]. For smaller values of N_F/N_0 , the fraction of recombined antiprotons tends to saturate by the time the positron temperature doubles. The saturation is understandable in consideration of the strong temperature dependence for three-body recombination.

It is possible to obtain an expression for the time dependence of the positron temperature by combining Eqs. (45) and (49). The expression is

$$t = \frac{3kn_F}{2n_0} \int_{T_0}^{T_t} \frac{dT}{(1-F_{\text{rec}})(dE/dt)}, \quad (50)$$

which must be numerically inverted to obtain T_t as a function of time t . Alternatively, a value for T_t can be chosen such that a desired value for F_{rec} is reached, and then the time it takes for T_t and the desired value of F_{rec} to be reached can be obtained. For example, using the same parameters as above ($n_F = 5 \times 10^{13} \text{ m}^{-3}$, $B = 2 \text{ T}$, a 3 eV antiproton kinetic energy, and $T_0 = 10 \text{ K}$) and assuming an initial antiproton density of $3 \times 10^9 \text{ m}^{-3}$, it is found to take 0.055 s for $F_{\text{rec}} = 0.5$ to be reached with $T_t = 10.16 \text{ K}$ and $N_F/N_0 = 10^4$. Note that the required time to reach $F_{\text{rec}} = 0.5$ is about an order of magnitude smaller than the antiproton slowing time scale calculated in the preceding section. Consequently, the assumption that the antiproton kinetic energy remains essentially unchanged during recombination is valid. For a second example, $t = 0.88 \text{ s}$ is obtained for $n_0 = 3 \times 10^9 \text{ m}^{-3}$, $F_{\text{rec}} = 0.5$, $T_t = 13 \text{ K}$, and $N_F/N_0 = 10^3$. In this case, the assumption that the antiproton kinetic energy remains essentially unchanged during recombination is not valid, and the calculations are not consistent. It should also be mentioned that in choosing an antiproton density, the antiproton plasma length must be larger than the positron plasma length so that the antiproton plasma completely overlaps the positron plasma (assuming the same plasma radius for the two plasmas). For example, a positron plasma consisting of 10^8 positrons with a density of $5 \times 10^{13} \text{ m}^{-3}$ and a cylindrical radius of 3 mm has a length of about 7 cm. An antiproton plasma consisting of 10^4 antiprotons with a density of $3 \times 10^9 \text{ m}^{-3}$ and a cylindrical radius of 3 mm has a length of about 12 cm, which satisfies the requirement. As a final note, it should be emphasized that the results of the present section do not take into account the possible detrimental effect of the presence of an electric field on three-body recombination.

IX. EFFECT OF ELECTRIC FIELD ON RECOMBINATION

A ‘‘threshold field’’ at which electric field ionization occurs for hydrogen Rydberg atoms with principal quantum numbers greater than n_{max} is given by [32]

$$E_{\text{th}} = \frac{e}{64\pi\epsilon_0 a_0^2 n_{\text{max}}^4}, \quad (51)$$

where $a_0 = 5.29 \times 10^{-11} \text{ m}$ is the Bohr radius. The radial electric field produced by a uniform cylindrical positron

plasma at locations far from the axial plasma edges is approximately given by Gauss' law as

$$E_r(r) = \frac{en_F r}{2\epsilon_0}, \quad (52)$$

provided the plasma length is much larger than the plasma diameter. Setting E_{th} equal to $E_r(r_{max})$ provides an expression for the maximum principal quantum number out to a maximum radius r_{max} within the plasma. The expression is

$$n_{max} = \left(\frac{1}{32\pi a_0^2 n_F r_{max}} \right)^{1/4}. \quad (53)$$

For example, for a 3 mm radius positron plasma having a $5 \times 10^{13} \text{ m}^{-3}$ density, principal quantum numbers up to 70 can be produced out to the plasma edge without being ionized by the plasma's electric field. For the same positron density, principal quantum numbers up to 100 can be produced out to $r_{max} = 0.7 \text{ mm}$.

The distribution of initial principal quantum numbers arising in three-body recombination may be expected to be proportional to the sixth power of the principal quantum number [20]. However, atoms that are initially recombined with too large a value for the principal quantum number become ionized (e.g., by the electric field in the plasma or by collisions). It is useful to define three transition values for the principal quantum number of an antihydrogen Rydberg atom. For the definitions, the atom is assumed to remain within a static positron plasma indefinitely, and the effect of the electric field produced by the plasma is neglected. Also, only collisional processes (e.g., collisional deexcitation, excitation, and ionization) are considered. First, n_1 is defined as the largest value for which a Rydberg atom has very close to 100% chance of remaining in a bound state indefinitely. For the second definition, n_2 is defined as the principal quantum number for which a Rydberg atom has about 50% chance of remaining in a bound state indefinitely. Third, n_3 is defined as the principal quantum number for which a Rydberg atom has very close to 100% chance of eventually being ionized. In Ref. [29], values for Rydberg energies associated with n_1 , n_2 , and n_3 are reported, which indicate $n_1 = 126/\sqrt{T}$, $n_2 = 180/\sqrt{T}$, and $n_3 = 397/\sqrt{T}$. The value of n_{max} relative to n_1 , n_2 , and n_3 gives an indication of the importance of electric field ionization of Rydberg atoms within the plasma. If n_{max} is larger than n_3 then the electric field may be considered unimportant since Rydberg atoms with principal quantum numbers larger than n_3 would be ionized even if the electric field were not present. For a 10 K positron plasma,

$n_1 = 40$, $n_2 = 57$, and $n_3 = 126$. These results indicate that the radial electric field produced by the plasma may be detrimental, and a more detailed assessment of the effect of an electric field on antihydrogen recombination is warranted.

X. CONCLUSION

A method for evaluating lower order Fokker-Planck coefficients has been developed. By using recent results from Ref. [11], the coefficients were reduced to exact onefold integrals. To avoid divergence of the integrals, a cutoff in the lower limit had to be introduced. The lower limit, which is proportional to the minimum change in test particle momentum during binary Coulomb collisions, was written in terms of the Coulomb logarithm. When combined with higher order Fokker-Planck coefficients, given by Eq. (15) [3], a complete set is formed for calculations of binary Coulomb scattering with Maxwellian field particles. When a weak coupling approximation was applied to the one-fold integrals, standard analytical expressions were recovered. Hence, a new approach to arriving at standard friction and diffusion coefficients was also obtained.

The expressions for the lower order Fokker-Planck coefficients are applicable for any value of the Coulomb logarithm. Motivated by this, the range of validity for several analytical expressions for the Coulomb logarithm was determined by comparison to numerical values. As an application of the theory, a time scale was predicted that describes the rate at which a reflecting antiproton beam slows down within a positron plasma with both species confined by a nested Penning trap. The Coulomb logarithm used in the calculation has a value of $\lambda = 0.00788$ and the time scale was found to be much larger than the time scale for recombination. Consequently, recombination may be possible for the parameters considered. To assess the possibility of achieving antihydrogen recombination in nested Penning traps in more detail, the effect of antiproton heating of the positrons was considered. It was found that a sizeable fraction of antiprotons would recombine provided the ratio of the number of confined positrons to the number of initially confined antiprotons was large enough for a given density of positrons. However, it was also found that the radial electric field produced by the plasma may limit the production of antihydrogen atoms to within a small region near the axis of symmetry of the plasma.

ACKNOWLEDGMENT

This material was based upon work supported by the National Science Foundation under Grant No. PHY-9876921.

-
- [1] F.L. Hinton, in *Basic Plasma Physics*, edited by A. A. Galeev and R. N. Sudan (North-Holland, New York, 1983), Vol. 1, p. 147.
- [2] C.-K. Li and R.D. Petrasso, *Phys. Rev. Lett.* **70**, 3063 (1993).
- [3] Y. Chang and D. Li, *Phys. Rev. E* **53**, 3999 (1996).
- [4] E.C. Shoub, *Phys. Fluids* **30**, 1340 (1987); E.C. Shoub, *Astrophys. J.* **389**, 558 (1992).
- [5] M. Psimopoulos, *Phys. Lett. A* **125**, 258 (1987); M. Psimopou-

- los and A. Rogister, *ibid.* **149**, 265 (1990).
- [6] C.A. Ordonez and M.I. Molina, *Phys. Plasmas* **1**, 2515 (1994).
- [7] E. Besuelle, R.R.E. Salomaa, and D. Teychenne, *Phys. Rev. E* **60**, 2260 (1999).
- [8] H. Risken, *The Fokker-Planck Equation: Methods of Solution and Applications* (Spring-Verlag, Berlin, 1984).
- [9] L.C. Woods, *Principles of Magnetoplasma Dynamics* (Clarendon, Oxford, 1987), Chap. 3.

- [10] D.C. Montgomery and D.A. Tidman, *Plasma Kinetic Theory* (McGraw-Hill, New York, 1964), Chap. 2.
- [11] Y. Chang and C.A. Ordóñez, *Phys. Plasmas* **6**, 2947 (1999).
- [12] Y. Chang, *Phys. Fluids B* **4**, 313 (1992); Y. Chang, Y. Huo, and G. Yu, *ibid.* **4**, 3621 (1992).
- [13] Y. Chang, Y.P. Huo, and J.X. Liu, *Commun. Theor. Phys.* **20**, 359 (1993).
- [14] P.J. Davis, in *Handbook of Mathematical Functions with Formulas, Graphs, and Mathematical Tables*, edited by M. Abramowitz and I. A. Stegun (Wiley, New York, 1972), p. 253.
- [15] C.A. Ordóñez, *Phys. Fluids B* **5**, 1367 (1993).
- [16] L. Spitzer, *Physics of Fully Ionized Gases* (Interscience, New York, 1962), Chap. 5.
- [17] M.E. Glinsky, T.M. O'Neil, M.N. Rosenbluth, K. Tsuruta, and S. Ichimaru, *Phys. Fluids B* **4**, 1156 (1992).
- [18] A.W. Hyatt, C.F. Driscoll, and J.H. Malmberg, *Phys. Rev. Lett.* **59**, 2975 (1987).
- [19] B.R. Beck, J. Fajans, and J.H. Malmberg, *Phys. Rev. Lett.* **68**, 317 (1992).
- [20] M.H. Holzscheiter and M. Charlton, *Rep. Prog. Phys.* **62**, 1 (1999).
- [21] G. Gabrielse, J. Estrada, S. Peil, T. Roach, J.N. Tan, and P. Yesley, in *Non-Neutral Plasma Physics III*, edited by J.J. Bollinger, R.L. Spencer, and R.C. Davidson, AIP Conf. Proc. No. 498 (AIP, Melville, 1999), p. 29, and references therein.
- [22] K.S. Fine, in *Non-Neutral Plasma Physics III* [21], p. 40.
- [23] C.A. Ordóñez, *Phys. Plasmas* **4**, 2313 (1997).
- [24] C.A. Ordóñez, *IEEE Trans. Plasma Sci.* **24**, 1378 (1996).
- [25] D.D. Dolliver and C.A. Ordóñez, *Phys. Rev. E* **59**, 7121 (1999).
- [26] D.S. Hall and G. Gabrielse, *Phys. Rev. Lett.* **77**, 1962 (1996).
- [27] D.D. Dolliver and C.A. Ordóñez, in *Non-Neutral Plasma Physics III* [21], p. 65.
- [28] G. Gabrielse, S.L. Rolston, L. Haarsma, and W. Kells, *Phys. Lett. A* **129**, 38 (1988).
- [29] M.E. Glinsky and T.M. O'Neil, *Phys. Fluids B* **3**, 1279 (1991).
- [30] P.O. Fedichev, *Phys. Lett. A* **226**, 289 (1997).
- [31] C.M. Surko, S.J. Gilbert and R.G. Greaves, in *Non-Neutral Plasma Physics III* [21], p. 3.
- [32] R.J. Damburg and V.V. Kolosov, in *Rydberg States of Atoms and Molecules*, edited by R.F. Stebbings and F.B. Dunning (Cambridge University Press, Cambridge, England, 1983), p. 31.